Title
A DIRECT EULERIAN MUSCL SCHEME FOR GAS DYNAMICS

Author
Colella, P.

Publication Date
1982-02-01

LBL-14104
Preprint

Lawrence Berkeley Laboratory
UNIVERSITY OF CALIFORNIA

Physics, Computer Science & Mathematics Division

Submitted for publication

A DIRECT EULERIAN MUSCL SCHEME FOR GAS DYNAMICS

Phillip Colella

February 1982

Prepared for the U.S. Department of Energy under Contract DE-AC03-76SF00098

DISCLAIMER

LBL-14104

A DIRECT EULERIAN MUSCL SCHEME FOR GAS DYNAMICS

Phillip Colella

Lawrence Berkeley Laboratory
University of California
Berkeley, California 94720

February 1982

This work was supported in part by the Director, Office of Basic Energy Sciences, Engineering, Mathematical, and Geosciences Division of the U.S. Department of Energy under contract DE-AC03-76SF00098.

A DIRECT EULERIAN MUSCL SCHEME FOR GAS DYNAMICS

Abstract

We present an extension to gas dynamics in Eulerian coordinates of MUSCL, van Leer's second order accurate generalization of Godunov's method for gas dynamics in Lagrangian coordinates. Unlike previous extensions to Eulerian coordinates, which calculated a Lagrangian step, followed by a remap, the present method performs the calculation in a single step by solving Riemann problems and characteristic equations for the fluxes in the Eulerian frame. We also make several simplifications in the formulation of the scheme, all aimed at making a more robust, and, in some ways, more accurate scheme. We present the results of test calculations in one and two space variables.

I. Introduction

In [7], van Leer described MUSCL, a second order accurate extension of Godunov's method ([4],[5]) for solving the gas dynamics in one space variable in Lagrangian coordinates. Van Leer presented this Lagrangian scheme as the core of a multidimensional Eulerian code, developed by van Leer and Woodward [8]. One time step of a one dimensional Eulerian calculation is done by performing a one dimensional Lagrangian step, then mapping the results back to a fixed Eulerian grid. The multidimensional algorithm is obtained by using the one dimensional Eulerian algorithm with operator splitting.

In this paper, we present a different MUSCL algorithm, based on some of the ideas in [7], for computing gas dynamics in Eulerian coordinates in one space dimension. The present algorithm is not formulated as a Lagrangian step, followed by a remap, but performs the Eulerian calculation in a single step. This direct Eulerian MUSCL bears the same relation to the nonlinear Eulerian Godunov algorithm discussed in [1],[5], as the Lagrangian MUSCL does to Godunov's method in Lagrangian coordinates. As in [7], the extension to multidimensional calculations is then performed using operator splitting.

Because we work in Eulerian coordinates, the engineering details are substantially different for the direct Eulerian scheme than for the Lagrangian scheme. In particular, dissipative mechanisms present in the latter are strongly diminished, if not totally absent, in the former, especially at places where one of the characteristic speeds vanishes. This, plus the additional logic involved with both solving the Riemann problem and tracing characteristics in the Eulerian frame, make for a slightly more complicated, but more accurate, algorithm than the simplest form of the 1D Lagrange plus remap MUSCL discussed in [7]. On the other hand, there is no remap to perform. Furthermore, we introduce some simplifications whose analogues are not present in the Lagrangian method In particular, we use the simplified Riemann problem solver

discussed in [1]. Also, we derive the slopes of the distributions of the dependent variables from the average values, rather than treating them as separate dependent variables, as was done in the code which generated the results presented in [7]. The interpolation algorithm for deriving the slopes is slightly more complicated than the second order central difference algorithm discussed in [7], but again yields more accurate results. Thus the present one dimensional algorithm is compatible with any multidimensional Eulerian code which performs its hydrodynamics calculation in a series of one-dimensional passes. In the end we find that the results obtained using the direct Eulerian algorithm are comparable to, if not somewhat better than, those obtained with the Lagrange plus remap code.

II. Description of the method

We will be constructing approximate solutions to Euler's equations describing the motion of an inviscid compressible fluid in one space variable r:

$$\frac{\partial U}{\partial t} + \frac{\partial (AF)}{\partial V} + \frac{\partial H}{\partial r} = 0$$

$$U = \begin{pmatrix} \rho \\ \rho u \\ \rho v \\ \rho E \end{pmatrix}$$

$$F(U) = \begin{pmatrix} \rho u \\ \rho u^2 \\ \rho uv \\ \rho uE + up \end{pmatrix} \qquad (2.1)$$

$$H(U) = \begin{pmatrix} 0 \\ p \\ 0 \\ 0 \end{pmatrix} .$$

Here $V = V(r)$ is a generalized volume coordinate, $A(r) = \frac{dV}{dr}$. These equations

describe one dimensional inviscid compressible flow with either planar, cylindrical, or spherical symmetry, or flow in a duct whose cross-section at r if A(r), depending on whether $V(r) = r$, $\frac{r^2}{2}$, $\frac{r^3}{3}$, or $\int_{r_0}^{r} A(r)dr$, respectively. Here ρ is the density, u is the component of velocity in the direction of the one-dimensional sweep, v is the component of velocity orthogonal to u (hereafter, u and v will be referred to as the velocity and transverse velocity, respectively), and E is the total energy per unit mass. We define e, the internal energy per unit mass, and p, the pressure, as

$$e = E - \frac{1}{2}(u^2+v^2) \qquad p = (\gamma-1)\rho e$$

where γ is the ratio of specific heats. Throughout this paper, γ will be assumed to be a constant, $\gamma>1$ (polytropic gas); for a discussion of the modifications required for a more general equation of state, see Colella and Glaz [2].

There are several other derived quantities which will be of interest: τ, the specific volume, c, the speed of sound, and $\lambda_{\pm,0}$, the three characteristic velocities:

$$\tau = \tau(U) = \frac{1}{\rho}$$

$$c = c(U) = \sqrt{\frac{\gamma p}{\rho}}$$

$$\lambda_\pm = \lambda_\pm(U) = u \pm c$$

$$\lambda_0(U) = u \quad .$$

Let Δt be a time increment, $r_{j+\frac{1}{2}}$ the boundary between zones j and $j+1$, and define $r_j = \frac{1}{2}(r_{j+\frac{1}{2}} + r_{j-\frac{1}{2}})$, $\Delta r_j = r_{j+\frac{1}{2}} - r_{j-\frac{1}{2}}$. We assume that, at time t^n, we know U_j^n, the averages of the conserved quantities across each zone:

$$U_j^n = \frac{1}{\Delta V_j} \int_{r_{j-\frac{1}{2}}}^{r_{j+\frac{1}{2}}} U(r,t^n)dV \, .$$

We wish to compute U_j^{n+1}, the averages of the conserved quantities at the new time $t^{n+1} = t^n + \Delta t$:

$$U_j^{n+1} = \frac{1}{\Delta V_j} \int_{r_{j-\frac{1}{2}}}^{r_{j+\frac{1}{2}}} U(r, t^{n+1}) dV .$$

In outline, the procedure followed by MUSCL for calculating U_j^{n+1} can be divided into five steps:

1) Compute linear profiles of the dependent variables in each zone by interpolating slopes at the centers of zones, subject to certain monotonicity constraints. This gives rise to a global distribution of the dependent variables which is piecewise linear, linear in each zone, with jump discontinuities at the edges of zones.

2) Compute $U_{j+\frac{1}{2}}^n$, the solution at the old time at the edges of zones, by solving the Riemann problems which resolve the jump discontinuities at the edges of the zones.

3) Compute $U_{j+\frac{1}{2}}^{n+1}$, an approximation to the solution at the edge of the zones at the new time, by tracing approximate characteristics, and solving difference approximations to the characteristic equations.

4) Compute time-averaged values of F and H, using the values computed in 2) and 3), and the following formula:

$$F_{j+\frac{1}{2}} = \frac{\Delta t}{2}(F(U_{j+\frac{1}{2}}^n) + F(U_{j+\frac{1}{2}}^{n+1})) = \int_{t^n}^{t^{n+1}} F(U(r_{j+\frac{1}{2}}, t)dt + O(\Delta t^3 + \Delta r_j^2 \Delta t)$$

$$H_{j+\frac{1}{2}} = \frac{\Delta t}{2}(H(U_{j+\frac{1}{2}}^n) + H(U_{j+\frac{1}{2}}^{n+1})) = \int_{t^n}^{t^{n+1}} H(U(r_{j+\frac{1}{2}}, t))dt + O(\Delta t^3 + \Delta t \Delta r_j^2)$$

5) Calculate the conserved quantities using divided differences of the values calculated in 4):

$$U_j^{n+1} = U_j^n - \frac{A_{j+\frac{1}{2}}F_{j+\frac{1}{2}} - A_{j-\frac{1}{2}}F_{j-\frac{1}{2}}}{\Delta V_j} - \frac{(H_{j+\frac{1}{2}} - H_{j-\frac{1}{2}})}{\Delta r_j} \qquad (2.2)$$

$$\Delta V_j = V(r_{j+\frac{1}{2}}) - V(r_{j-\frac{1}{2}})$$

Clearly, most of the work in this algorithm is in steps 1) - 3). We will proceed to describe those steps in more detail.

Step 1: Interpolation of Slopes

Given our discrete data U_j^n, we will interpolate a global description for our dependent variables at all points (r,t^n) which is piecewise linear, and linear in each zone:

$$q(r) = q_j^n + \delta q_j \frac{(r-r_j)}{\Delta r_j} \tag{2.3}$$

$$r_{j-\frac{1}{2}} < r < r_{j+\frac{1}{2}}$$

Here $q = q(U)$ represents any useful flow variable, conserved or not. For $q = p,\rho,u,v$, we will take $q_j^n = q(U_j^n)$, and construct the slopes δq_j by a suitable difference formula. The distributions of other quantities $s = s(p,\rho,u,v)$ are then derived from those of p,ρ,u,v in the following fashion:

$$q_{j+\frac{1}{2},L} = q_j^n + \tfrac{1}{2}\delta q_j \quad , q_{j+\frac{1}{2},R} = q_{j+1}^n - \tfrac{1}{2}\delta q_{j+1} \qquad q = p,\rho,u,v$$

$$s_{j+\frac{1}{2},S} = s(p_{j+\frac{1}{2},S},\rho_{j+\frac{1}{2},S},u_{j+\frac{1}{2},S},v_{j+\frac{1}{2},S}) \quad S = L,R$$

$$\delta s_j = (s_{j+\frac{1}{2},L} - s_{j-\frac{1}{2},R})$$

$$s_j^n = \frac{1}{2}(s_{j+\frac{1}{2},L} + s_{j-\frac{1}{2},R})$$

$$s(r) = s_j^n + \delta s_j \frac{(r-r_j)}{\Delta r_j} \qquad r_{j-\frac{1}{2}} < r < r_{j+\frac{1}{2}} \tag{2.4}$$

In the case of equally spaced zones $\Delta r_j = \Delta r$, δq_j is calculated using the following two-step algorithm. We first calculate $\delta_f q_j$, a first guess to the slope using the

monotonized central difference algorithm discussed in [7].

$$\delta_{\lim} q_j = \min(|q_{j+1}^n - q_j^n|, |q_j^n - q_{j-1}^n|) \cdot 2 \text{ if } (q_{j+1}^n - q_j^n)(q_j^n - q_{j-1}^n) > 0$$
$$= 0 \quad \text{otherwise}$$

$$\delta_f q_j = \min\left(\frac{|q_{j+1} - q_{j-1}|}{2}, \delta_{\lim} q_j\right) \times sgn(q_{j+1} - q_{j-1}) . \tag{2.5}$$

Finally, we calculate δq_j by differencing the values at two points on either side of r obtained by using the interpolant given using $\delta_f q$ as the slope:

$$\delta q_j = \min\left\{\frac{2}{3}|q_{j+1} - \frac{1}{4}\delta_f q_{j+1} - q_{j-1} - \frac{1}{4}\delta_f q_{j-1}|, \delta_{\lim} q_j\right\} sgn(q_{j+1} - q_{j-1})$$

$$\delta q_j = \delta(q_{j-2}, \ldots, q_{j+2}) \tag{2.6}$$

To obtain δq_j in the case of unequal zones, calculate $\bar{\delta} q_j = \delta(q_{j-2}, \ldots, q_{j+2})$, $\bar{\delta} r_j = \delta(r_{j-2}, \ldots, r_{j+2})$, using (2.6) . Then we calculate

$$\delta q_j = \Delta r_j \min\left\{\frac{|\bar{\delta} q_j|}{|\bar{\delta} r_j|}, \frac{2|q_{j+1} - q_j|}{\Delta r_j}, \frac{2|q_j - q_{j-1}|}{\Delta r_j}\right\} sgn(q_{j+1} - q_{j-1}) \tag{2.7}$$

In the case where the minima in (2.5)-(2.7) are obtained in the first arguments, one obtains

$$\frac{\delta q_j}{\Delta r_j} = \frac{\left[\frac{2}{3}(q_{j+1} - q_{j-1}) - \frac{1}{12}(q_{j+2} - q_{j-2})\right]}{\left[\frac{2}{3}(r_{j+1} - r_{j-1}) - \frac{1}{12}(r_{j+2} - r_{j-2})\right]}$$

which is a fourth order finite difference approximation to $\frac{dq}{dr}|_{r_j}$, and thus is well behaved in regions where the solution is smooth. The fact that δq_j is obtained from $\delta_f q$, a monotonized first guess, gives rise to steeper profiles representing discontinuities than those obtained using either the fourth-order accurate formula by itself, or by setting $\delta q_j = \delta_f q_j$, as was suggested in [7].

There are situations, however, in which the above slope setting procedure leads to profiles which are too steep, in the sense that the scheme will not provide sufficient dissipation to ensure that the correct amount of shock heating occurs. This situation arises when the speed of the characteristic of the family associated with the shock changes sign across the shock, i.e., where the shock is nearly stagnant. In such situations, the calculation remains stable, but there is a small amplitude ($\lesssim 5\%$), low frequency error in the post shock values generated at the shock. In this case, we reduce the slopes computed by the above procedure by some fraction S_j, $0 \le S_j \le 1$: $\delta q_j^{reduced} = \delta q_j S_j$. We want S_j to have the following properties If the j^{th} zone is not inside a shock, or if the j^{th} zone is inside the shock, but the speed of the characteristics of the family associated with that shock doesn't change sign, then $S_j = 1$. If the j^{th} zone is inside a shock having zero velocity, then $S_j = 0$, thus reducing the method locally to Godunov's method. Intermediate cases should have an intermediate amount of flattening. Finally, $S_j = 1$ if there is not the possibility of a significant amount of shock heating across the zone. The formula given below for S_j satisfies the above requirements.

$$W_j^2 = |p_{j+1} - p_{j-1}| \Big/ \left| \frac{1}{\rho_{j+1}} - \frac{1}{\rho_{j-1}} \right|$$

$$\mathbf{s}_j = sgn(p_{j-1} - p_{j+1})$$

$$\lambda_{j,+} = u_{j+1} + \mathbf{s}_j c_{j+1}, \quad \lambda_{j,-} = u_{j-1} + \mathbf{s}_j c_{j-1}$$

$$U_j = \frac{W_j}{\rho_{j+\mathbf{s}_j}} + \mathbf{s}_j \, u_{j+\mathbf{s}_j}$$

$$\overline{S}_j = \frac{|U_j|}{|U_j| + min(|\lambda_{j,+}|, |\lambda_{j,-}|)}$$

$$\text{if } \varepsilon_p - \frac{|p_{j+1} - p_{j-1}|}{min(p_{j+1}, p_{j-1})}, \ \lambda_{j,+} \lambda_{j,-}, \text{ and } (u_{j+1} - u_{j-1}) < 0$$

= 1 otherwise

$$S_j = max(0, 1-(1-\bar{S}_j)/\eta) .$$

Here $0 < \eta \leq 1$ and ε_p is the minimum pressure jump which would be considered a shock; in the calculations presented here $\eta = \frac{1}{2}$, $\varepsilon_p = \frac{1}{4}$.

Steps 2-3: Calculation of Interface Values

We must calculate $U^n_{j+\frac{1}{2}}, U^{n+1}_{j+\frac{1}{2}}$, approximate values to the solution at the old and new times, at the zone edges $r_{j+\frac{1}{2}}$. To obtain $U^n_{j+\frac{1}{2}}$, we calculate the solution to the Riemann problem (for a detailed discussion, see Colella [1], and the references cited there). As is well known, the solution to the Riemann problem with left and right states U_L, U_R is $h(\frac{r}{t}, U_L, U_R)$; i.e., it depends on r, t only in the ratio $\frac{r}{t}$.

To calculate $U^n_{j+\frac{1}{2}}$, we take our states

$$U_L \ , \ U_R = U^n_{j+\frac{1}{2},L} \ , \ U^n_{j+\frac{1}{2},R}$$

(see figure 1), and set

$$U^n_{j+\frac{1}{2}} = h(0; U_L, U_R) .$$

If $U^n(r,t)$ is the exact solution to the initial value problem given by the global piecewise linear distribution (2.3), then $\lim_{t \downarrow t^n} U^n(r_{j+\frac{1}{2}}, t) = U^n_{j+\frac{1}{2}}$.

As was the case for the Eulerian Godunov's method, the approximate Riemann problem solver described in [1] appears to be both inexpensive and sufficiently accurate, without introducing rarefaction shocks into the solution.

To calculate U^{n+1}_j, we solve a finite difference approximation to the characteristic equations, which we review briefly below. Given a solution $U(x,t)$ to (2.1), we say that a curve $\sigma_{\pm,0} \rightarrow (r(\sigma_{\pm,0}), t(\sigma_{\pm,0}))$ is a characteristic of the +,-,0 family if U is continuous in a

neighborhood of that curve, and if the following ordinary differential equations hold

$$\frac{dr}{d\sigma_{\pm,0}} = \lambda_{\pm,0} \qquad \frac{dt}{d\sigma} = 1 \quad (2.8)_{\pm,0}$$

$$\frac{1}{\rho c}\frac{dp}{d\sigma_\pm} \pm \frac{du}{d\sigma_\pm} + \frac{A'}{A}uc = 0 \qquad (2.9)_\pm$$

$$\frac{d\tau}{d\sigma_0} = -\frac{1}{(\rho c)^2}\frac{dp}{d\sigma_0} \qquad (2.9)_0 .$$

Here $\frac{ds}{d\sigma} = \frac{d}{d\sigma}(s(r(\sigma),t(\sigma)))$ and all functions of (r,t) are evaluated at $(r(\sigma),t(\sigma))$.

The equations (2.8),(2.9) completely describe the solution in regions where U is continuous or near contact discontinuities. However, in the neighborhood of a shock, the equations (2.9) no longer hold along the curves described by (2.8), and some modification to the equations must be introduced which takes into account this fact.

Our strategy for calculating $U^{n+1}_{j+\frac{1}{2}}$ proceeds as follows, considering, for the moment, the case $\frac{dA}{dr} \equiv 0$. First, we find approximations to the paths described by $(2.8)_{\pm,0}$ which intersect the point $(r_{j+\frac{1}{2}}, t^{n+1})$, taking due care to trace backwards to the origins of centered rarefaction fans if $(r_{j+\frac{1}{2}}, t)$ $t > t^n$ is inside such a fan. Then we calculate $U^{n+1}_{j+\frac{1}{2}}$ in three stages. First, we solve a pair of nonlinear algebraic equations for $p^{n+1}_{j+\frac{1}{2}}$, $u^{n+1}_{j+\frac{1}{2}}$, given the values of the solution at the base of the +,- characteristics. These are the same nonlinear algebraic equations as those for the values of p,u between the two sonic waves in the Riemann problem with left and right states, given by, respectively, the values of the solution at the base of the + and - characteristics. Intuitively, what we are doing is lumping all the waves of the + (resp -) family which are crossed by the - (resp +) characteristic into a single shock or rarefaction shock jump. In the case where the solution is continuously differentiable, we obtain a nonlinear finite difference approximation to $(2.9)_\pm$. If the solution is not smooth, this procedure gives values for $p^{n+1}_{j+\frac{1}{2}}$, $u^{n+1}_{j+\frac{1}{2}}$ which are well behaved. We then solve an explicit equation for the $\rho^{n+1}_{j+\frac{1}{2}}$, given the value of the solution at time t^n and that of $p^{n+1}_{j+\frac{1}{2}}$, which again

lumps the pressure wave crossing the streamline into a single shock or rarefaction shock. In the limit that the pressure jump is small, we similarly obtain a solution to a finite difference approximation to $(2.9)_0$. Finally, $v_{j+\frac{1}{2}}^{n+1}$ is just set equal to its value at the base of the approximate characteristic of the 0-family.

We now give the details of the procedure outlined above. First, we want to determine points $(r_{j+\frac{1}{2},\#}, t^n)$ such that $(r_{j+\frac{1}{2},\#}, t^n)$ and $(r_{j+\frac{1}{2}}, t^{n+1})$ are connected by a straight line which approximates a solution to $(2.8)_\#$. To this end, we define $\Delta r^{tr}_{j+\frac{1}{2},\#}$, $\mathbf{s}^{tr}$, $r^{tr}_{j+\frac{1}{2},\#}$; $q^{tr}_{j+\frac{1}{2},\#}$, $\delta q^{tr}_{j+\frac{1}{2},\#}$, $q = p, \rho, u, v, \lambda_\#$, as follows:

$$(q^{tr}_{j+\frac{1}{2},\#}, \delta q^{tr}_{j+\frac{1}{2},\#}, \Delta r^{tr}_{j+\frac{1}{2},\#}, \mathbf{s}^{tr}_{j+\frac{1}{2},\#}) = (q_{j-1}, \delta q_{j-\frac{1}{2}}, \Delta r_{j-1}, r_{j-1}, 1) \text{ if } \lambda_\#(U^{n+1}_{j+\frac{1}{2}}) \geq \varepsilon^\#$$

$$= (q_j, \delta q_j, \Delta r_j, r_j, -1) \text{ if } \lambda_\#(U^{n+1}_{j+\frac{1}{2}}) < -\varepsilon^\#$$

These are the quantities which describe the linear distribution of the dependent variables in the zone which contains $(r_{j+\frac{1}{2},\#}, t^n)$. Throughout this discussion, we will take $\varepsilon^\pm = \varepsilon > 0$, $\varepsilon^0 = 0$, where ε is chosen such that $|\lambda_\#(U^n_{j+\frac{1}{2}})| < \varepsilon^\#$ implies that the value of the solution to the Riemann problem at $(r_{j+\frac{1}{2}}, t^n)$ being taken on inside a centered rarefaction fan of the # family. In that case, we use a different procedure, tracing characteristics of the # family back to the Riemann problem originating at $(r_{j+\frac{1}{2}}, t^n)$.

$$d = \frac{-\frac{1}{2}\mathbf{s}^{tr}_{j+\frac{1}{2},\#} + \lambda^{tr}_{j+\frac{1}{2},\#}\dfrac{\Delta t}{\Delta r^{tr}_{j+\frac{1}{2},\#}}}{1 + \delta\lambda^{tr}_{j+\frac{1}{2},\#}\dfrac{\Delta t}{\Delta r^{tr}_{j+\frac{1}{2},\#}}}$$

$$r_{j+\frac{1}{2},\#} = r_{j+\frac{1}{2}} - \mathbf{s}^{tr}_{j+\frac{1}{2},\#} max(\, min(\, d\,,\, \tfrac{1}{2}\,)\,,\, -\tfrac{1}{2}\,)\Delta r^{tr}_{j+\frac{1}{2},\#} \qquad (2.10)$$

In the case where the maxima and minima are obtained in their first arguments, this is a formula for the point where a straight line with slope $\lambda_\#(\, r_{j+\frac{1}{2},\#}\,)$ passing through the point $(r_{j+\frac{1}{2}}, t^{n+1})$ intersects the line $\{t = t^n\}$ (figure 2). If we were integrating a single conservation law, this line would coincide exactly with the characteristic through $(r_{j+\frac{1}{2}}, t^{n+1})$, given that the characteristic velocity had the linear distribution

given by (2.4). To the extent that we use (2.10) for a system, we are neglecting the effect of the interaction between waves of different families on the wave speeds in tracing the characteristics. This introduces an $O(\Delta r^{tr}_{j+\frac{1}{2},\#}\Delta t)$ error into the value of $r_{j+\frac{1}{2},\#}$. The maxima and minima which appear in (2.10) constitute a convenient choice for $r_{j+\frac{1}{2},\#}$ for certain pathological cases which occasionally occur in the course of the calculation.

Given $r_{j+\frac{1}{2},\#}$ we can also define $q_{j+\frac{1}{2},\#}$, the value of the solution at the base of the # characteristic passing through $(r_{j+\frac{1}{2}}, t^{n+1})$:

$$q_{j+\frac{1}{2},\#} = q(r_{j+\frac{1}{2},\#}) = q^{tr}_{j+\frac{1}{2},\#} + \frac{r_{j+\frac{1}{2},\#} - r^{tr}_{j+\frac{1}{2},\#}}{\Delta r^{tr}_{j+\frac{1}{2},\#}} \delta q^{tr}_{j+\frac{1}{2},\#}$$

$$q = p, \rho, u, v \ .$$

In the case where $|\lambda^n_{\#,j+\frac{1}{2}}| < \varepsilon^{\#}$, we assume that the characteristic of that family passing through $(r_{j+\frac{1}{2}}, t^n)$ originates from the Riemann problem at $(r_{j+\frac{1}{2}}, t^n)$, and we define $r_{j+\frac{1}{2},\#}$, $q_{j+\frac{1}{2},\#}$ accordingly:

$$r_{j+\frac{1}{2},\#} = r_{j+\frac{1}{2}}, \quad q_{j+\frac{1}{2},\#} = q^n_{j+\frac{1}{2}} \qquad q = p, \rho, u, v \ . \tag{2.11}$$

Given $q_{j+\frac{1}{2},\#}$, $q = p, \rho, u, v$, $\# = 0, +, -$, we can now express $p^{n+1}_{j+\frac{1}{2}}$, $\rho^{n+1}_{j+\frac{1}{2}}$, $u^{n+1}_{j+\frac{1}{2}}$, $v^{n+1}_{j+\frac{1}{2}}$ in terms of those quantities. First, we require that $p^{n+1}_{j+\frac{1}{2}}, u^{n+1}_{j+\frac{1}{2}}$ satisfy the pair of equations

$$\frac{(p^{n+1}_{j+\frac{1}{2}} - p_{j+\frac{1}{2},\pm})}{W(p^{n+1}_{j+\frac{1}{2}}, p_{j+\frac{1}{2},\pm}, \rho_{j+\frac{1}{2},\pm})} \pm (u^{n+1}_{j+\frac{1}{2}} - u_{j+\frac{1}{2},\pm}) = 0 \tag{2.12}$$

$$W(p^*, p, \rho) = (\gamma p \rho (1 + \frac{\gamma+1}{2\gamma} \frac{p^* - p}{p}))^{\frac{1}{2}} .$$

If $|p_{j+\frac{1}{2},+} - p_{j+\frac{1}{2}}|$, $|u_{j+\frac{1}{2},+} - u_{j+\frac{1}{2}}|$ are $O(\Delta r_j$, $\Delta r_{j+1})$, then this is just a finite difference approximation to $(2.9)_{\pm}$. If either the quantities $|p_{j+\frac{1}{2},+} - p_{j+\frac{1}{2},-}|$, $|u_{j+\frac{1}{2},-} - u_{j+\frac{1}{2},+}|$ is O(1), then we have the interpretation of the equations (2.12) given above. The equations (2.12) for p^{n+1}, u^{n+1} are exactly the ones given in [1] for the central pressure and velocity for the approximate Riemann problem solver given in [1], and the iteration

scheme given there can be used to solve (2.12) for p^{n+1}, u^{n+1}.

The values for $\rho_{j+\frac{1}{2}}^{n+1}, v_{j+\frac{1}{2}}^{n+1}$ are given by the following explicit expressions:

$$\rho_{j+\frac{1}{2}}^{n+1} = \left[\frac{1}{\rho_{j+\frac{1}{2},0}} - \frac{(p_{j+\frac{1}{2}}^{n+1} - p_{j+\frac{1}{2},0})}{W(p_{j+\frac{1}{2}}^{n+1}, p_{j+\frac{1}{2},\pm}, \rho_{j+\frac{1}{2},\pm})^2}\right]^{-1} \tag{2.13}$$

$$v_{j+\frac{1}{2}}^{n+1} = v_{j+\frac{1}{2},0} .$$

In the case where $A' \neq 0$, we want to include the effect of the source terms in the calculation of $p^{n+1}, \rho^{n+1}, u^{n+1}, v^{n+1}$. Let $\bar{p}^{n+1}$, $\bar{u}^{n+1}$, be the values obtained by the procedure leading up to the equations (2.12) i.e., not including the effect of source terms. We obtain $p_{j+\frac{1}{2}}^{n+1}$, $u_{j+\frac{1}{2}}^{n+1}$, by solving the following set of linear equations, which approximate $(2.9)_{\pm}$

$$\frac{1}{W_{\pm}}(p_{j+\frac{1}{2}}^{n+1} - p_{j+\frac{1}{2},\pm}) \pm (u_{j+\frac{1}{2}}^{n+1} - u_{j+\frac{1}{2},\pm}) + \frac{A'(r_{j+\frac{1}{2},\pm})}{A(r_{j+\frac{1}{2},\pm})} u_{j+\frac{1}{2},\pm} c_{j+\frac{1}{2},\pm} = 0$$

Where $W_{\pm} = W(\bar{p}_{j+\frac{1}{2}}^{n+1}, p_{j+\frac{1}{2},\pm}, \rho_{j+\frac{1}{2},\pm})$ and $c_{j+\frac{1}{2},\pm} = c(r_{j+\frac{1}{2},\pm})$ have already been obtained above in calculating the solution without source terms.. After a little algebra, one finds

$$p_{j+\frac{1}{2}}^{n+1} = \bar{p}_{j+\frac{1}{2}}^{n+1} - \left[\frac{A'(r_{j+\frac{1}{2},+})}{A(r_{j+\frac{1}{2},+})} u_{j+\frac{1}{2},+} c_{j+\frac{1}{2},+} + \frac{A'(r_{j+\frac{1}{2},-})}{A(r_{j+\frac{1}{2},-})} u_{j+\frac{1}{2},-} c_{j+\frac{1}{2},-}\right] \Delta t \frac{W_+ W_-}{W_+ + W_-}$$

$$u_{j+\frac{1}{2}}^{n+1} = \bar{u}_{j+\frac{1}{2}}^{n+1} + \frac{\Delta t}{W_+ + W_-}\left[\frac{W_- A'(r_{j+\frac{1}{2},-})}{A(r_{j+\frac{1}{2},-})} u_{j+\frac{1}{2},-} c_{j+\frac{1}{2},-} - \frac{W_+ A'(r_{j+\frac{1}{2},+})}{A(r_{j+\frac{1}{2},+})} u_{j+\frac{1}{2},+} c_{j+\frac{1}{2},-}\right] \tag{2.14}$$

Given $p_{j+\frac{1}{2}}^{n+1}$, $u_{j+\frac{1}{2}}^{n+1}$ the values for the other variables are obtained using (2.13)

This completes the calculation of $U_{j+\frac{1}{2}}^{n}$, $U_{j+\frac{1}{2}}^{n+1}$. These are then inserted into (2.2) to obtain the U_j^{n+1}, the conserved quantities at the new time. The time step Δt must satisfy the usual CFL condition for in order to insure stability:

$$\Delta t \leq \sigma \max_j \left(\frac{\Delta r_j}{|u_j^n| + c_j^n}\right) \tag{2.15}$$

Where $0 < \sigma < 1$. The smallest σ for which (2.15) is satisfied is called the CFL number for that time step of the calculation.

III. Numerical Results

Boundary Conditions

In order to calculate U_j^{n+1}, $j = M_L, \ldots, M_R$, it suffices to specify q_j^n, $(\delta q)_j$, $j = M_L-1, \ldots, M_R+1$. Then one has sufficient data to calculate $U_{j+\frac{1}{2}}^n$, $U_{j+\frac{1}{2}}^{n+1}$, $j = M_L-1, \ldots, M_R$, and the U_j^{n+1}'s. If we can specify q_j^n, $j = M_L-3, \ldots, M_R+3$, then it follows from (2.6) that we can calculate δq_j, $j = M_L-1, \ldots, M_R+1$. In one dimension, or for two-dimensional problems for which the boundaries are aligned with the mesh directions, this is straightforward. For example, for the left boundary, we have

Reflecting Wall: $q_{M_L-l} = q_{M_L+l-1}$, $l = 1,2,3$, $q = \rho, p, v$; $u_{M_L-l} = -u_{M_L-l-1}$

Continuation: $q_{M_L-l} = q_{M_L+l-1} q = \rho, p, u, v$, $l = 1,2,3$,

Inflow: $q_{M_L-l}^n = q_0(t^n)$, $l = 1,2,3$, $q = p, \rho, u, v$, $q_0(t)$ given.

For a reflecting wall, we have chosen to change the slope limiting procedure slightly. We allow the values extrapolated to the wall to take on the values which are obtained at the wall by solving a Riemann problem with left and right states $(U_L, U_R) = (U_{M_L-1}^n, U_{M_L})$. This procedure seems to improve the resolution of shock reflections in multidimensional calculations.

Specifically, if we define p_{lim} to be one of the roots of

$$u_{M_L}^2 W(p_{\text{lim}}, p_{M_L}, \rho_{M_L})^2 - (p_{\text{lim}} - p_{M_L})^2 = 0 \tag{3.1}$$

where p_{lim} is the root $\lessgtr p_0$ if $u_{M_L} \lessgtr 0$. Then we define

$$u_{\text{lim}} = 0, \quad p_{\text{lim}} = \left(\frac{1}{\rho_{M_L}} - \frac{p_{\text{lim}} - p_{M_L}}{W^2} \right)^{-1}.$$

These are used in the equations for $\delta_{\lim} q_{M_L, M_{L-1}}$, $q = p, \rho, u$.

$$\delta_{\lim} q_{M_L} = min\left(2|q_{M_L} - q_{M_L+1}|,\ 2|q_{M_L} - q_{\lim}|\right) \text{ if } (q_{M_L} - q_{\lim})(q_{\lim} - q_{M_L+1}) > 0$$

$$= 0 \text{ otherwise}$$

$$\delta_{\lim} q_{M_L-1} = min\left(2|q_{M_L} - q_{M_L-1}|,\ 2|q_{M_L} - q_{\lim}|\right) \text{ if } (q_{M_L} - q_{\lim})(q_{\lim} - q_{M_L-1}) > 0$$

$$= 0 \text{ otherwise}$$

The corresponding procedure for a reflecting wall at M_R is obtained by exchanging $>, <$ in choosing the root of (3.1), and replacing M_L+1, M_L, M_L-1 with M_R-1, M_R, M_R+1.

If $u_{M_L-\frac{1}{2}}$ is the axis of symmetry for a cylindrically or spherically symmetric problem, then we treat it as a reflecting wall, except that the geometric source terms $\pm uc\ \frac{A'}{A}$ in the characteristic equations (2.9) are set equal to zero in calculating $U^{n+1}_{M_L-\frac{1}{2}}$, i.e., $\bar{q}^{n+1}_{M_L-\frac{1}{2}} = q^{n+1}_{M_L-\frac{1}{2}}$.

Finally, in the diverging duct problem discussed below, we use a characteristic boundary condition at the right-hand side of the duct. The density ρ_0 is specified to be a constant at the right end of the duct. Then, as a function of time values of p, u are specified using the characteristic equations, using the assumption that the $-,0$ characteristics point to the right:

$$\rho_{M_R+1} = \rho_0$$

$$u_{M_R+j} = u_{M_R} - \frac{(p_{M_R+j} - p_{M_R})}{\overline{\rho c}} \tag{3.2}$$

$$p_{M_R+1} = \left(\frac{p_{M_R}}{\rho_0}\right)^{\gamma} p_{M_R}$$

$$\overline{\rho c} = \frac{1}{2}\left(\sqrt{\rho_{M_R} p_{M_R} \gamma} + \sqrt{\rho_{M_R+j} p_{M_R+j} \gamma}\right)$$

Test Problems

This method has been tested on a variety of test problems in one space dimension, including shock tubes in Cartesian, cylindrical and spherical geometry. Results were obtained for one dimensional problems which were indistinguishable from those shown in [7] and [1], obtained using the Lagrange plus remap MUSCL. This method has also been used to calculate the oblique reflection of a shock against an inclined plane in two space variables [11], successfully resolving multiple Mach stem configurations.

We present here two test calculations. As a one-dimensional test problem, we calculated the steady state solution to the duct flow problem in Shubin, Stephens, and Glaz [6], marching in time until the steady state was reached. The duct is specified by $A(r) = 1.398 + .347\ tanh(.8r - 4)$, $0 \le r \le 10$, with boundary conditions

$$p(0,t) = .3809\ ,\ \rho(0,t) = .502\ ,\ u(0,t) = 1.299\ ;\ \rho(10,t) = .776\quad t \ge 0$$

The initial conditions are given by setting $q(x,0) = q(0,0)$, i.e., impulsive start. Inflow boundary conditions are imposed at the left boundary, and the characteristic boundary conditions (3.2) are imposed at the right boundary. The density profiles at $t = 200$ are shown in figure 3, for $\Delta r = \frac{1}{16}$ and $\Delta r = \frac{1}{32}$, plotted as a dotted line, with circles at the data points. This is to be compared with the exact solution, plotted as a solid line. We obtain good agreement with the exact solution, even for the coarsely zoned calculation.

We also calculated the two dimensional Cartesian shock reflection problem used by van Leer [7] as a test problem for the Lagrange plus remap versions of MUSCL; see also Woodward and Colella [8]. The computational domain is a channel of length 3 in the x direction, and of width 1 at the left end in the y direction, with a step of height .2 extending to the right beginning at x=.6 . The step and the upper and lower walls of the channel are reflecting boundaries, with a Mach 3 uniform inflow on the left, and continuation boundary conditions on the right. The initial conditions are that of uniform

flow throughout the channel:

$$p(x,y,0)=1\ ,\ \rho(x,y,0) = 1.4\ ,\ u_x(x,y,0) = 3\ ,\ u_y(x,y,0) = 0$$

In figures 4 and 5, we show the pressure and density contours of the solution at $t = 4$, with $\Delta x = \Delta y = .1$ and $.05$, respectively. The first shock reflection point along the upper wall has been seen in other calculations to be a Mach reflection, located directly above the edge of the step. The present calculations obtain the correct location of the reflection point, although the Mach stem in the $\Delta x = .1$ is two zones long; consequently, the slip line extending to the right from the triple point is not resolved, as it is in the $\Delta x = .05$ calculation. The other reflected shocks are well resolved in both calculations, even though they are quite weak.

These results represent an improvement over the the results in [7] in two respects. First, the overall resolution of the shocks, particularly in the $\Delta x = .1$ calculation, is substantially better. Second, the numerical boundary layer generated at the corner along the upper surface of the step is far weaker than that generated in the Lagrange plus remap results. In the latter calculation, the boundary layer separates at $x = 1$, changing somewhat the shock pattern downstream. The numerical boundary layer does not separate in the present calculations.

These two dimensional problems were run on the Cray I at LLNL using a fully vectorized implementation of the algorithm, the $\Delta x = .1$ calculation taking .066 minutes to run 194 time steps, and the $\Delta x = .05$ calculation taking .36 minutes to run 376 time steps. However, the vector lengths in these calculations were that of the number of zones in a one dimensional sweep, and were hence too short to observe the full speed of a fully vectorized calculation on the Cray. A more typical speed for larger problems is 20 μs / zone / time step / dimension.

IV. Discussion and Conclusions

The direct Eulerian MUSCL algorithm described above follows the basic conceptual framework given by van Leer for the Lagrangian MUSCL scheme. There are, however, substantial technical differences, all aimed at producing a more robust, and in certain ways, simpler scheme. A central feature to the engineering of the scheme is that of solving the characteristic equations (2.8)-(2.9) directly, rather, as in [7], than deriving a formula based on Taylor expansions, for the time derivative of the flux. The present approach makes it much easier to account correctly for sonic points in rarefaction waves (2.11), to introduce tracing characteristics forward in time (2.10); and to exploit the duality between the Riemann problem and the characteristic equations for gas dynamics by introducing the nonlinear algorithm for calculating $U^{n+1}_{j+\frac{1}{2}}$. The latter two procedures were essential for calculating strong shocks with CFL numbers close to 1, and appear to be necessary for Lagrangian calculations using MUSCL as well [10].

We have presented here the basic framework for extending the Lagrangian algorithm of van Leer to Eulerian gas dynamics. This approach can be easily modified to an arbitrary moving coordinate system, in one dimension, or a moving rectangular coordinate system in more than one dimension. A central issue which remains to be fully resolved for this method, as well as other higher order extensions of Godunov's method is controlling the behavior of such schemes when one of the characteristic speeds, measured relative to the mesh motion, vanishes. The treatment of sonic centered rarefaction waves and the flattening of slopes at stagnant shocks constitute a first step, but more work is required. A fuller analysis of these problems will appear in [3], along with some proposals for ameliorating them.

Acknowledgments. The author wishes to thank Paul Woodward for many helpful discussions, and Bram van Leer for a critical reading of the manuscript. The author also wishes to thank the Theoretical Physics Division at LLNL for making available the time on the LLNL Cray I. This work was supported in part by the Director, Office of Basic Energy Sciences, Engineering, Mathematical, and Geosciences Division of the U.S. Department of Energy under contract DE-AC03-76SF00098.

References

[1] Colella, P., "Glimm's method for gas dynamics", SISSC, in press.

[2] Colella, P., and Glaz, H.M., "Efficient solution algorithms for the Riemann problem for real gases", in preparation.

[3] Colella, P., and Woodward, P.R., "The piecewise parabolic method for gas-dynamical simulations", in preparation.

[4] Godunov, S.K., Mat. Sb. *47*, 271 (1959).

[5] Godunov, S.K., Zabrodyn, A.W., and Prokopov, G.P., Zhur. Vycisl. Mat. Fiz. *1*, 1020 (1961).

[6] Shubin, G.R., Stephens, A.B., and Glaz, H.M., J. Comp. Phys. *39*, 364 (1981).

[7] van Leer, B., J. Comp. Phys. *32*, 101 (1979).

[8] van Leer, B., and Woodward, P.R., Proc. TICOM Conf., Austin, Texas (1979).

[9] Woodward, P.R., and Colella, P., Lecture Notes in Physics *141*, 434 (1979).

[10] Woodward, P.R., private communication.

[11] Colella, P., and Glaz, H.M., "Calculation of complex shocked flows using a direct Eulerian MUSCL algorithm", paper presented at the 5th AIAA CFD Conference, Palo Alto, CA, June 1981.

Figure Captions

Figure 1. Spatial distribution of q at initial time t^n.

Figure 2. Approximate solution to the characteristic equation of the # family.

Figure 3. Steady state density profiles for one dimensional duct problem: a) $\Delta x = \frac{1}{16}$ b) $\Delta x = \frac{1}{32}$.

Figure 4. Contour plots for two dimensional test problem, $\Delta x = .1$. a) Density, 30 contours between .98 and 6.38. b) Pressure, 30 contours between 1.11 and 11.6.

Figure 5. Contour plots for two dimensional test problem, $\Delta x = .05$. a) Density, 30 contours between .68 and 6.29. b) Pressure, 30 contours between .72 and 11.8.

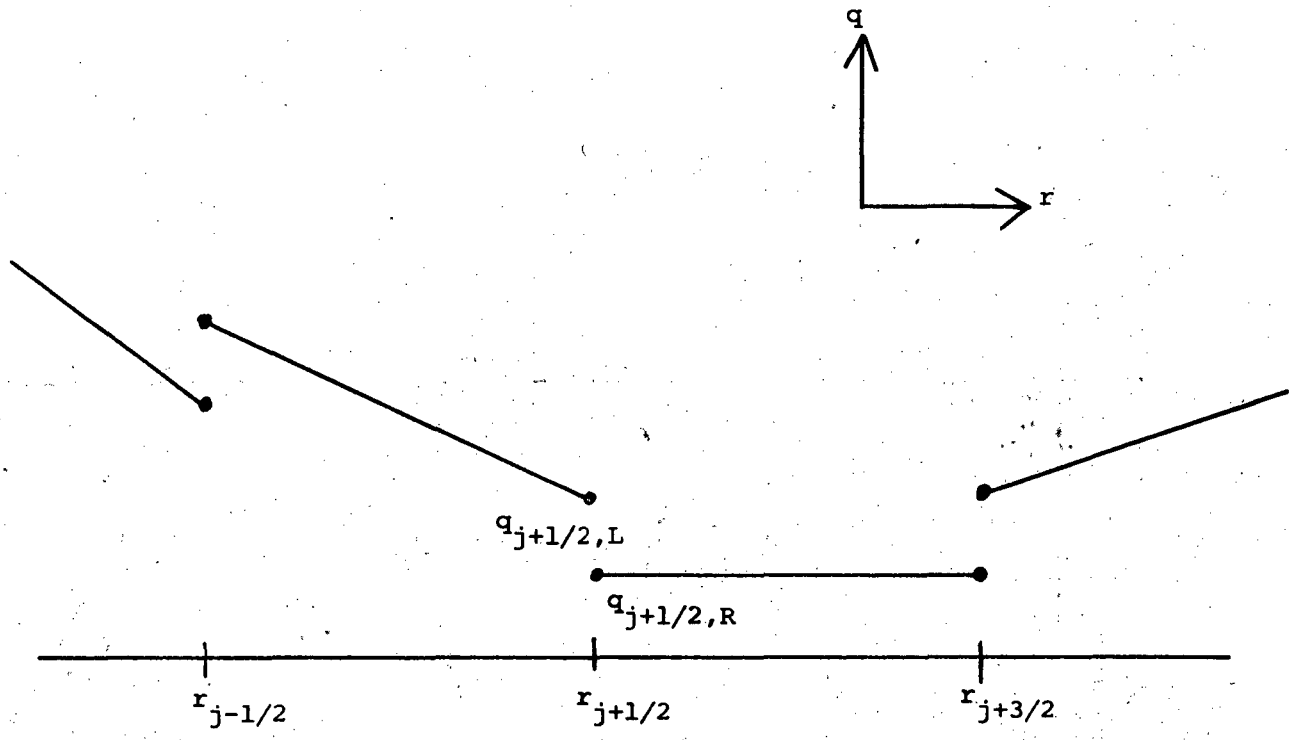

figure 1.

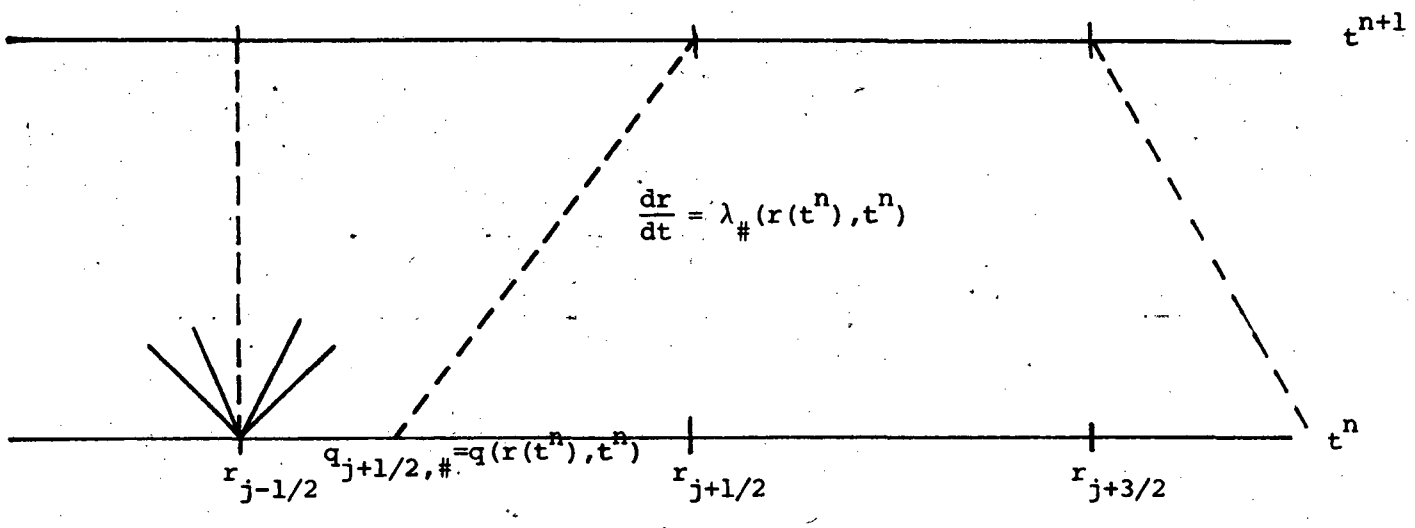

figure 2.

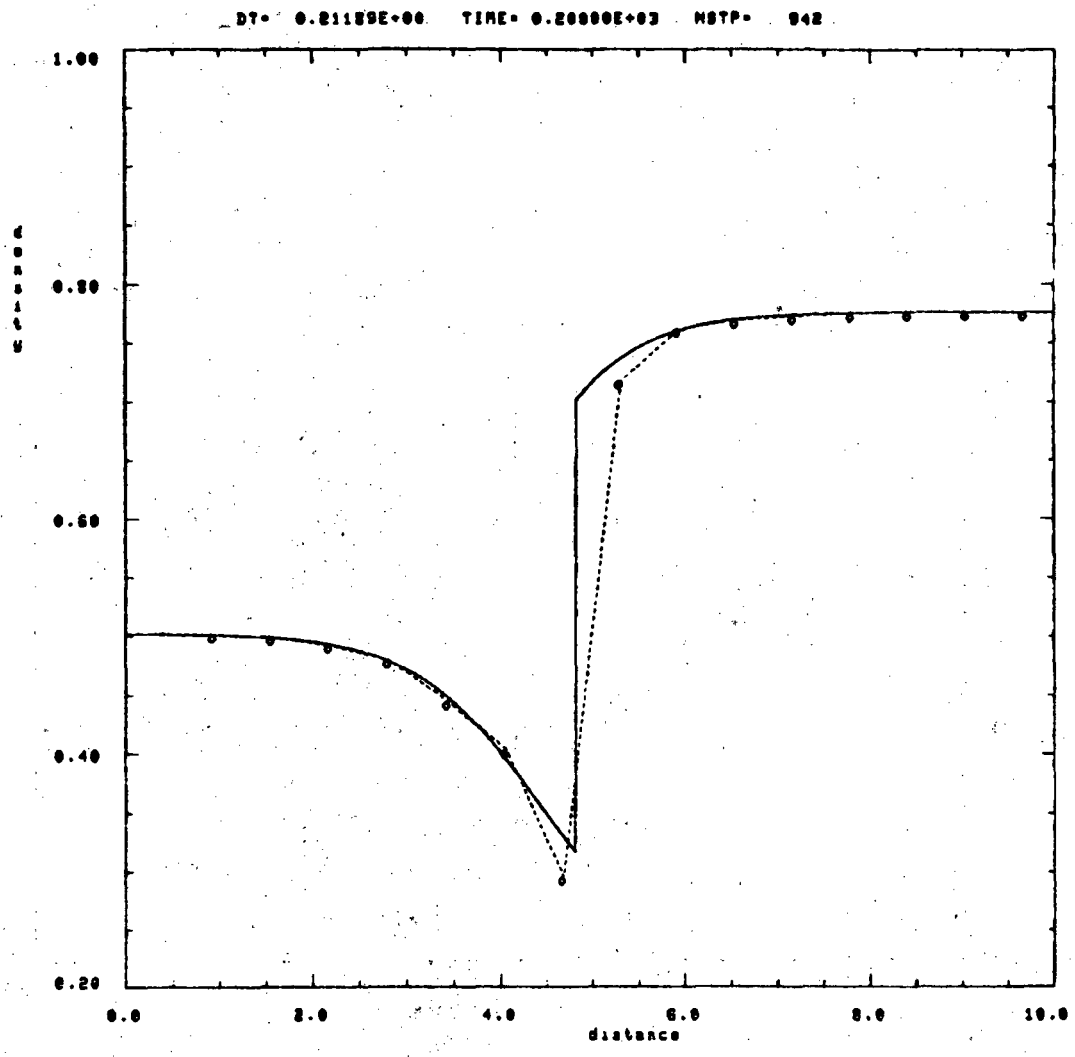
DT= 0.21189E+00 TIME= 0.20000E+01 NSTP= 942
1.00
0.80
0.60
0.40
0.20
density
0.0
2.0
4.0
6.0
8.0
10.0
distance

figure 3 a)

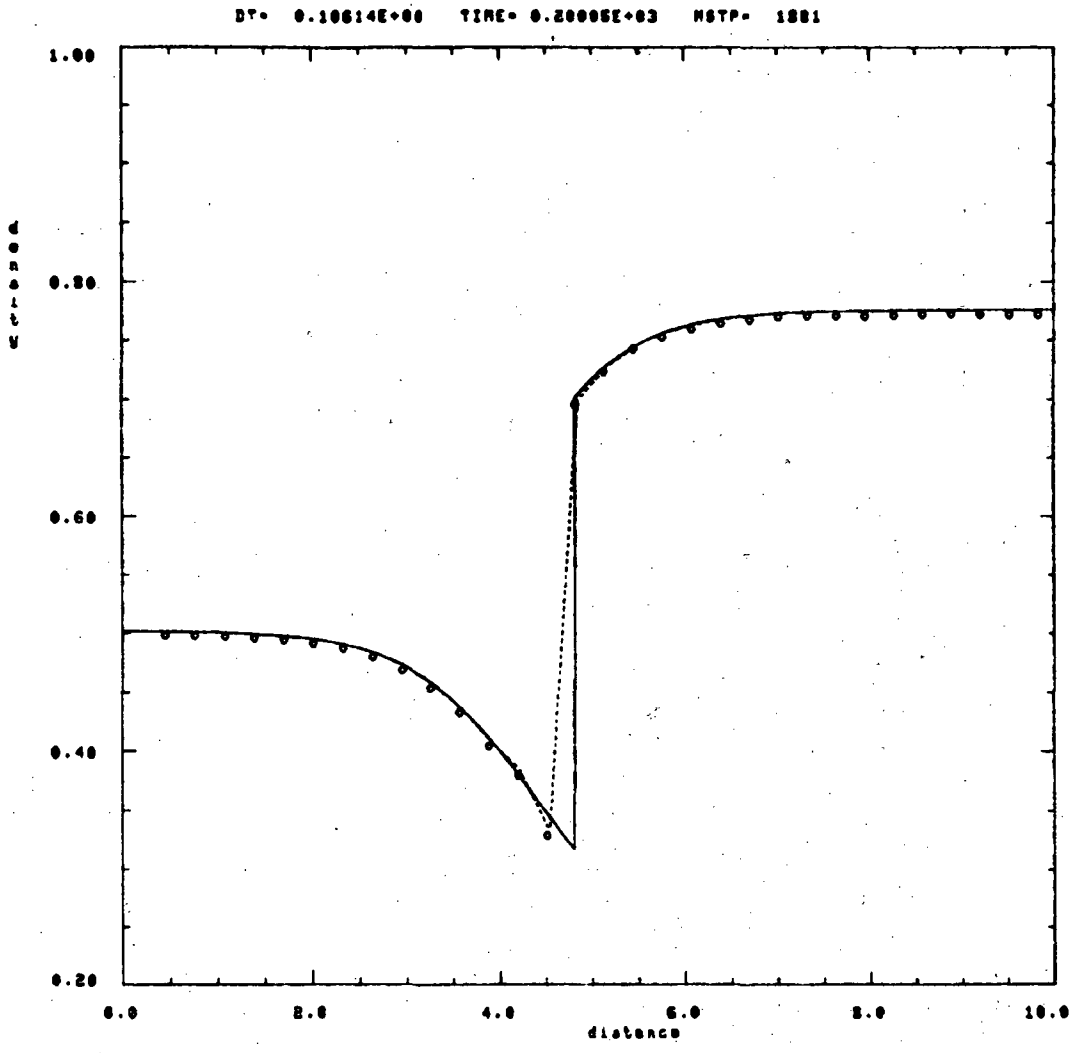
DT= 0.10614E+00 TIME= 0.20005E+03 NSTP= 1881
1.00
0.80
0.60
0.40
0.20
density
0.0
2.0
4.0
6.0
8.0
10.0
distance

figure 3 b)

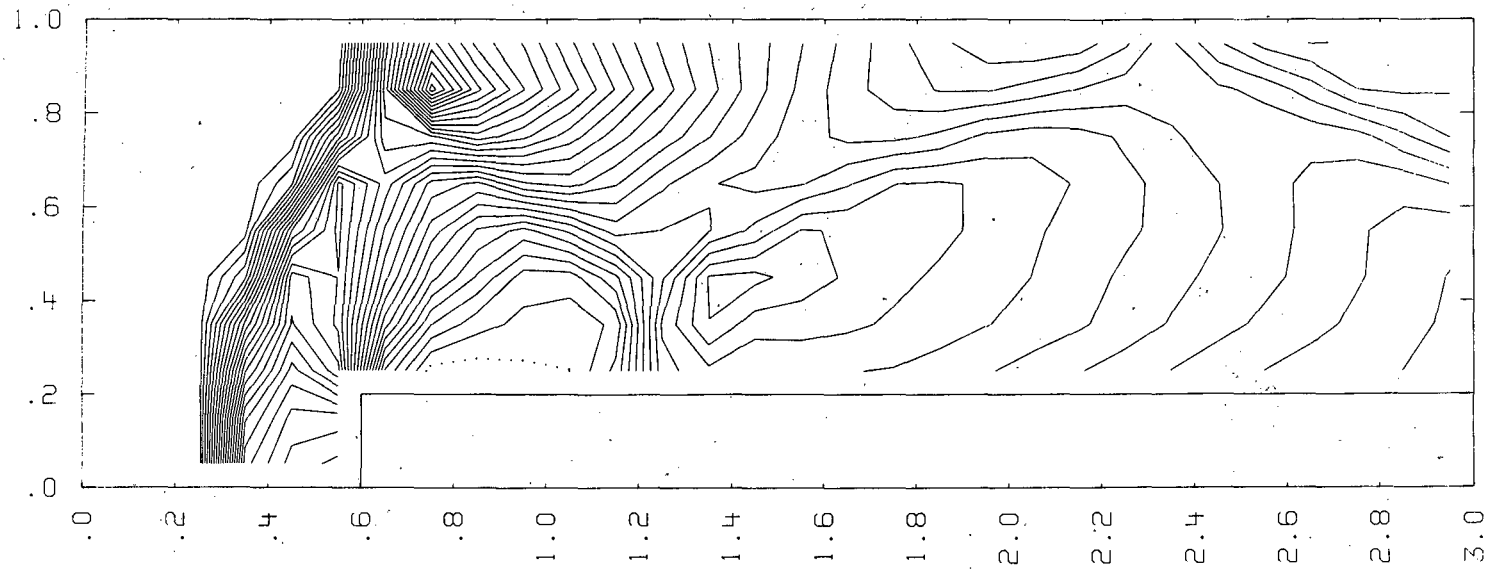

figure 4 a)

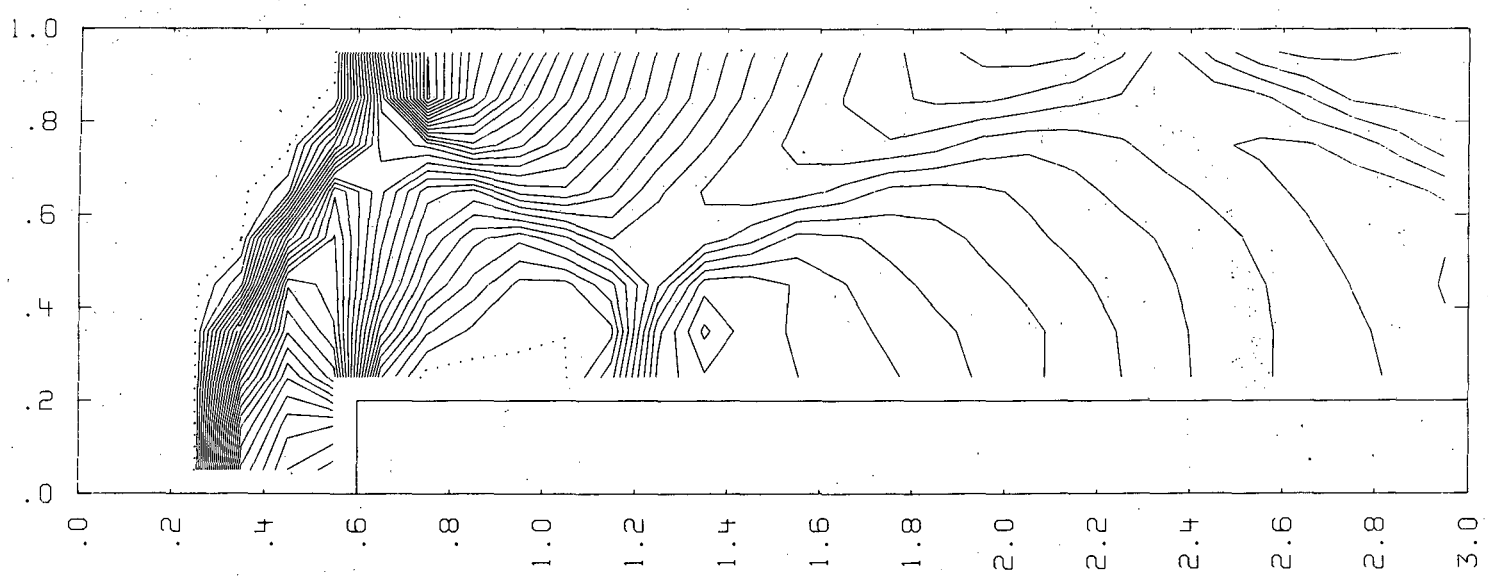

figure 4 b)

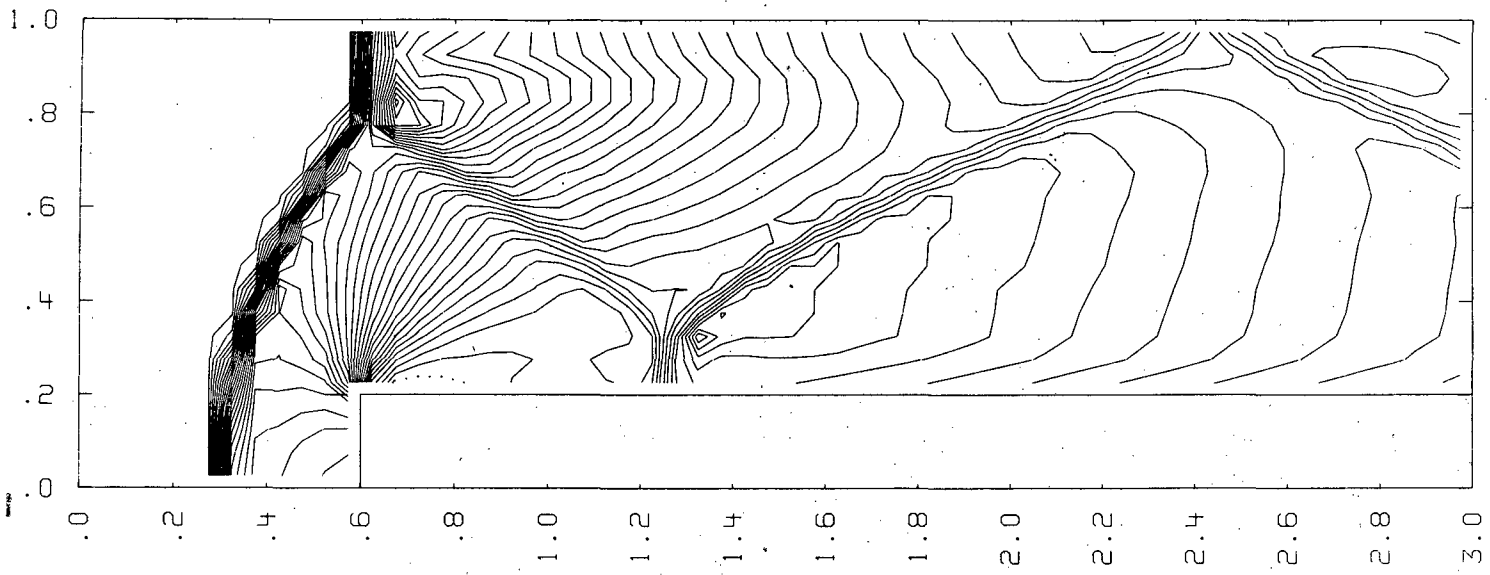

figure 5 a)

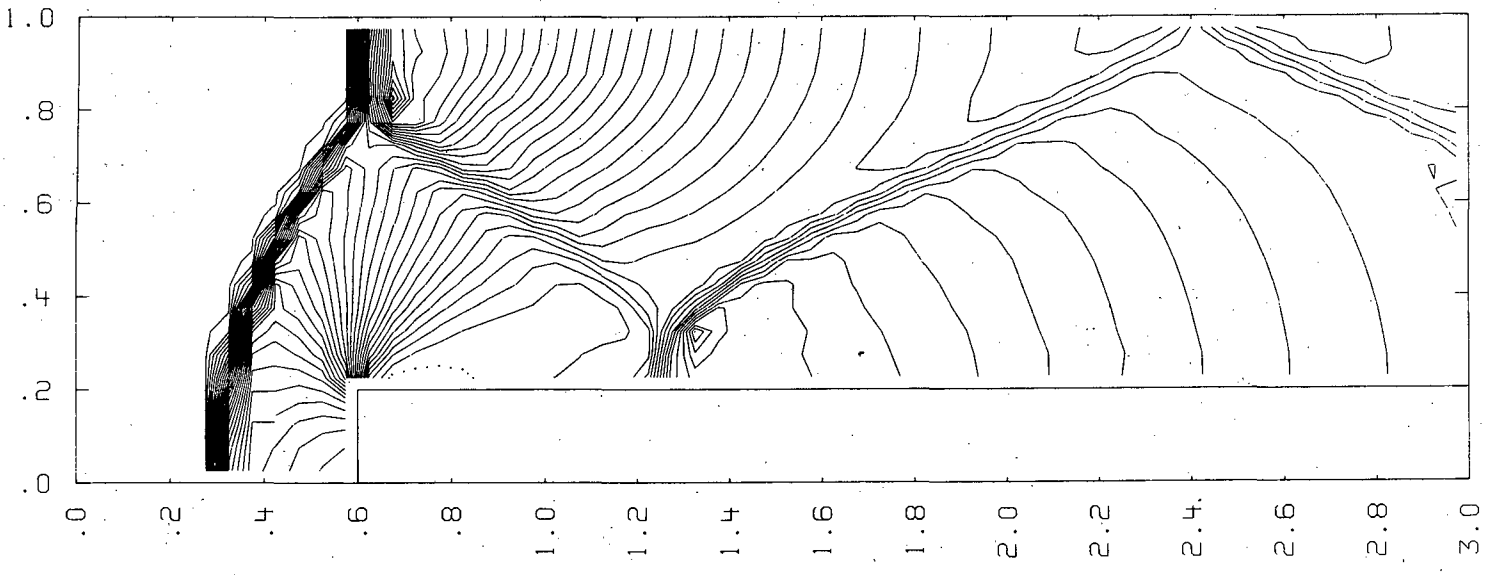

figure 5 b)

TECHNICAL INFORMATION DEPARTMENT
LAWRENCE BERKELEY LABORATORY
UNIVERSITY OF CALIFORNIA
BERKELEY, CALIFORNIA 94720